Assessing Macroscopic Fundamental Diagram Shapes for Bi-Modal Grid Networks

Namrata Gupta[a, *] and Ludovic Leclercq[a]

[a]*Univ Gustave Eiffel, ENTPE, LICIT-ECO7, F-69675 Lyon, France*

Keywords:
Bi-modal urban network
Macroscopic fundamental diagram
Dedicated Bus Lanes

Macroscopic Fundamental Diagram (MFD) is a widely recognized tool for evaluating and managing urban transportation networks by relating aggregate traffic variables such as flow, density, and speed. Predicting MFDs for new network configurations is critical for proactive transportation planning and operation. Achieving this requires a detailed understanding of how network topology influences MFD shapes. This study investigates bi-modal urban transportation networks, focusing on square grid configurations with Dedicated Bus Lanes (DBLs). Using a large sample of simulations in SUMO, we examine the sensitivity of MFDs to variations in intersection density, block lengths, and the number and placement of DBLs. Our findings reveal that even uniformly distributed DBLs introduce spatial heterogeneity in car networks, as DBL links reduce available lane space for cars. This heterogeneity significantly impacts MFD shapes, highlighting the limitations of spatially aggregated metrics and emphasizing the need for spatially aware topology quantification to better capture multimodal interactions.

1 Introduction

The Macroscopic Fundamental Diagram (MFD) is a valuable tool for understanding and managing urban transportation networks. By relating aggregate traffic variables such as flow, density, and speed across an urban road network, the MFD provides insights into system-wide performance. Throughout this study, the term ”MFD” refers to the relationship between average network flow and average network density. Over the past decades, this framework has been widely applied to research in various aspects of transportation, including routing (Knoop et al., 2012; Yildirimoglu and Geroliminis, 2014), congestion pricing (Zheng et al., 2012; Simoni et al., 2015), perimeter gating (Keyvan-Ekbatani et al., 2013; Haddad et al., 2013; Ortigosa et al., 2015; Li et al., 2021), traffic signal control (Zhang et al., 2013; Lu et al., 2020; Gupta et al., 2023, 2024), parking management (Geroliminis, 2015; Gu et al., 2021), and emergency evacuation

* Corresponding author. E-mail address: namrata.gupta@univ-eiffel.fr.

planning (Zhang et al., 2015). Zhang et al. (2020) and Johari et al. (2021) summarizes the recent developments in traffic flow modeling using MFDs. Given its utility, the estimation and prediction of MFDs have become active areas of research in transportation systems engineering.

A key area of ongoing research focuses on estimating MFDs for modified or new urban networks. While estimation based on real-world data—such as loop detectors (Buisson and Ladier, 2009), floating cars (Geroliminis and Daganzo, 2008), or a combination of both (Leclercq et al., 2014; Ambühl and Menendez, 2016)—makes characterization of existing networks easier, the ability to predict MFDs for hypothetical or future network configurations is equally essential. Such predictions are crucial for proactive planning, enabling policymakers to evaluate the impacts of infrastructural or demand changes before implementation. Achieving accurate MFD predictions requires identifying the network features that significantly influence MFD shapes.

To this end, Knoop et al. (2014) and Taillanter et al. (2024) investigates impact of network structures on MFDs using microsimulations; Mühlich et al. (2015) and Xu and Gayah (2023) examines the influence of hierarchical urban street networks on MFD hysteresis; and Loder et al. (2019) establishes relationships between network production, critical densities, and aggregate topological metrics using real-world data from 40 cities.

This study investigates bi-modal transportation networks, where cars and buses share the infrastructure. Specifically, we focus on networks with Dedicated Bus Lanes (DBLs), which are commonly implemented in urban areas to enhance public transport efficiency. For simplicity, buses are assumed to travel exclusively on DBLs. Using the SUMO traffic simulation platform, we analyze bi-modal square grid networks with varying numbers of intersections, block lengths, DBL counts, and DBL placement patterns. The primary objective is to assess the impact of DBLs on the MFDs of car networks, with a particular emphasis on understanding the spatial heterogeneity introduced by DBLs and its influence on network performance.

The remainder of this paper is structured as follows. Section 2 describes the simulation setup and experimental design, followed by the presentation and discussion of key results in Section 3. Finally, Section 4 summarizes the key insights.

2 Simulation experiment designs

We conduct our experiments using SUMO to simulate a bi-modal, bi-directional urban square grid network with two lanes per street. The network configurations are varied by adjusting the number of intersections in each direction (n) and the block length (L). Bus networks are incorporated by converting the right lanes of selected streets into DBLs, ensuring that DBLs are also added in the reverse direction for consistency with practical scenarios. For simplicity, buses travel exclusively on DBLs without mixed traffic conditions. The patterns for adding DBLs are illustrated in Figure 1, where an equal number of bus arterials are distributed in both horizontal and vertical directions. Table 1 summarizes the design parameters considered in our simulations.

All intersections are signalized, and we employ SUMO's default *gap-based actuated traffic control*[1] with two signal phases: one for eastbound and westbound movements, and the other for northbound and southbound movements. The maximum speeds of cars and buses are set at $40.00\,\mathrm{m/s}$ and $25.00\,\mathrm{m/s}$, respectively, while all other bus and car driving parameters use SUMO's default values. To ensure the

[1] Sumo documentation on traffic lights

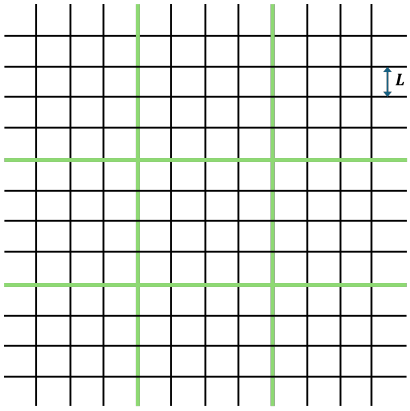

Figure 1: *Example of a network topology with 11 intersections ($n = 11$) and uniform placement of two bi-directional DBLs ($DBL = 2$) in each direction. Green lines indicate the DBL locations.*

system reaches a steady state, cars are loaded gradually into the network, minimizing sensitivity to total incoming demand and isolating the effects of network topology. Buses are generated at the network boundary with a fixed headway of 5 minutes.

Table 1: *Network generation parameters*

Symbol	Range	Description
n	$\{7, 11, 17\}$	Number of intersections in each direction
L	$\{300, 500\}$ m	Block length
DBL	$\begin{cases} \{0,1,2,3,7\} & \text{if } n = 7 \\ \{0,1,2,3,5,11\} & \text{if } n = 11 \\ \{0,1,2,4,5,17\} & \text{if } n = 17 \end{cases}$	Number of DBL uniformly placed in each direction

For route generation, we use SUMO's in-built *jtrrouter*[2] method to create random routes, with 20 % of vehicles turning right and 10 % turning left at all intersections during each timestep. All network boundaries are treated as feasible destinations, allowing vehicles to exit the network at its edges.

3 Results and discussion

In this section, we present the simulation results of different network. Each simulation setting is conducted with five different random seeds. The MFD shapes shown in the following discussion are averages of five different random seeds.

3.1 Effect of intersections and block length

To isolate the effect of intersections and block length, we simulated unimodal networks with varying numbers of intersections and block lengths. Figure 2a illustrates the MFDs for three intersection configurations

[2]Sumo documentation on jtrrouter

with a block length of 300 m. The results reveal that (i) the capacity and the density range at which capacity is achieved decrease with an increasing number of intersections, and (ii) congestion onset occurs at lower densities as the number of intersections increases. Figures 2b to 2d show the impact of block length for different number of intersections. The figures indicate that the free-flow branches have higher slopes for larger block length. Other than free-flow region, the effects of increased block length are similar but less pronounced compared to those of a reduced number of intersections. Moreover, a comparison of Figures 2b to 2d reveals that the benefits of longer block lengths vary with the number of intersections. The improvement in the density range at which capacity is achieved is more pronounced for $n = 11$ and less significant for $n = 17$.

Loder et al. (2019) analyzes the data from 40 cities and demonstrates that critical accumulation—the number of vehicles at which capacity is reached—is inversely related to intersection density. Note that block length is inversely proportional to intersection density. Thus, our findings in Figures 2b to 2d align with this conclusion. However, our results emphasize that the number of intersections has a more dominant effect on network performance than intersection density. This observation underscores the need to develop a more refined parameter than intersection density to accurately capture the effects of intersection interactions on network performance.

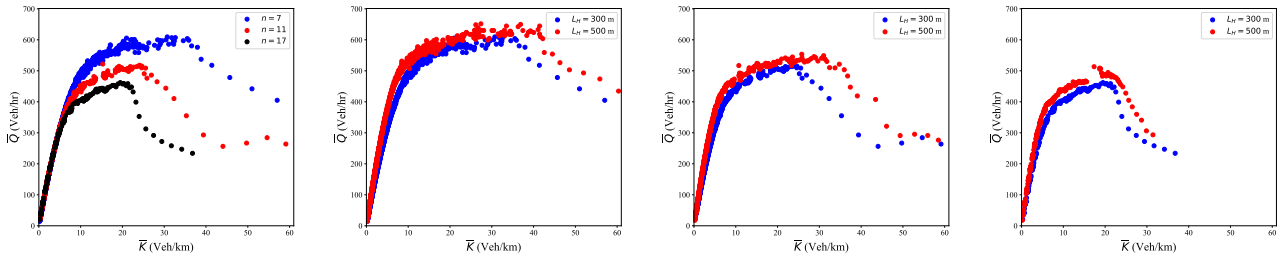

(a) *Block length of* 300 m **(b)** *Effect of block length for* $n = 7$ **(c)** *Effect of block length for* $n = 11$ **(d)** *Effect of block length for* $n = 17$

Figure 2: *Impact of intersections and block lengths on the MFD of unimodal networks (DBL* $= 0$*).*

3.2 Effect of DBLs

Figure 3a, Figure 3b, and Figure 3c depict the variation in MFD shapes for car networks with DBLs for $n = 7$, $n = 11$, and $n = 17$, respectively, when the block length is 300 m. These figures illustrate that the number of bus arterials influences the optimality region by affecting both the maximum average network flow and the critical density range at which capacity is achieved. The results reveal that introducing bus lanes creates a more complex impact than a simple monotonic degradation of capacity, highlighting intricate interactions between bus and car networks as buses and cars share capacity at intersections.

The spatial features contributing to these complexities are further analyzed. The placement of DBLs reduces the space available for cars and introduces spatial heterogeneity into the car network. With all streets having two lanes, the presence of DBLs limits certain streets to only one lane for car traffic. To better understand the patterns observed in Figure 3, we separately aggregate traffic parameters for links with one lane available for cars (due to DBLs) and for links without DBLs (both lanes available for cars). Since the patterns are consistent across all values of n, we focus on $n = 11$ to examine the changes in MFD shapes following DBL placement.

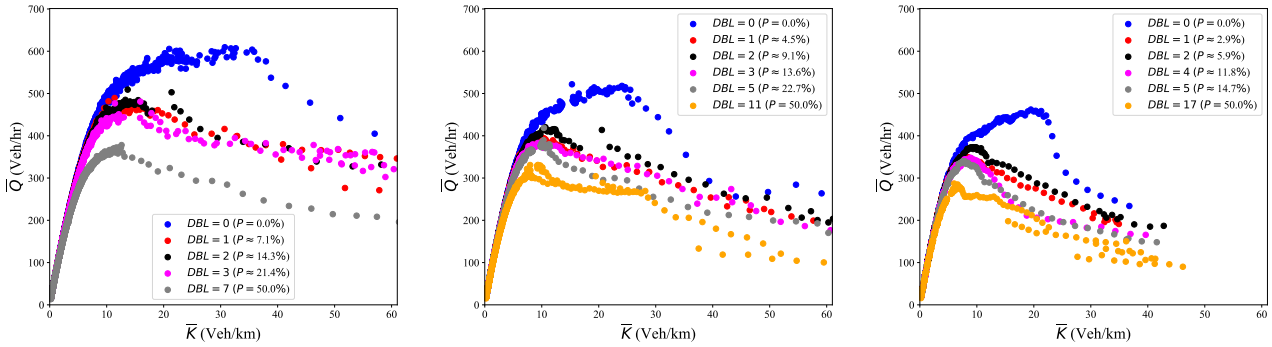

(a) $n = 7$ **(b)** $n = 11$ **(c)** $n = 17$

Figure 3: *MFD of the network available for cars. Network parameters:* $L = 300\,\text{m}$. *The variable P in legend represents the percentage of bus lanes in the network.*

Figure 4 and Figure 5 illustrate the aggregation of traffic parameters for links with DBLs (one lane for cars) and links without DBLs (both lanes for cars). These figures show the MFD shapes for car traffic alone. For links with DBLs (Figure 4), the MFD shapes change with an increasing number of DBLs. For a smaller number of DBLs, the MFD shape is closer to trapezoidal (Figure 4a). As the number of DBLs increases, the critical density range narrows, and the shape becomes closer to triangular (Figure 4d). Similar to unimodal networks, the slope of the free-flow branch is higher for networks with larger block lengths, but the MFDs for both block lengths overlap outside the free-flow region.

In contrast, the MFD shapes for links without DBLs (Figure 5) are triangular for all configurations. Unlike in unimodal cases (Figures 2b to 2d), in some cases, the congested branch of the MFD exhibits higher flow for smaller block lengths. While this observation requires further investigation, it suggests that in multi-modal networks, the relationship between block length and MFD shapes may differ from that in unimodal traffic.

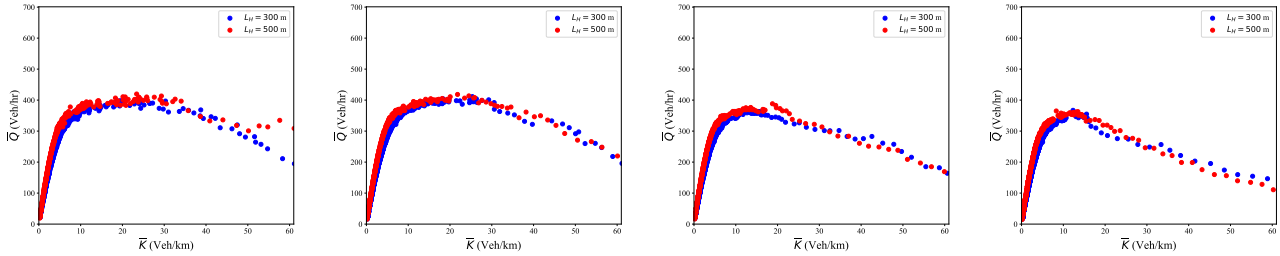

(a) $DBL = 1$ **(b)** $DBL = 2$ **(c)** $DBL = 3$ **(d)** $DBL = 5$

Figure 4: *MFD of links where one lane is available for cars. Network parameters:* $n = 11$.

The bus arterials also contribute to variations in intersection characteristics within the car network. To investigate whether the locations of intersections with DBLs influence the car network's MFD, we created multiple network topologies for $DBL = 1$ by offsetting the bus arterials' positions by an offset value O from the center. Figure 6a illustrates an example of such a network with $n = 11$, $DBL = 1$, and $O = 2$. Figure 6b demonstrates that the placement of bus lines impacts the car network's MFD. The MFD shapes are shown for a block length of 300 m, but similar results were observed for $L = 500\,\text{m}$; these are not included here for brevity. These findings underscore the sensitivity of car network performance to DBL locations.

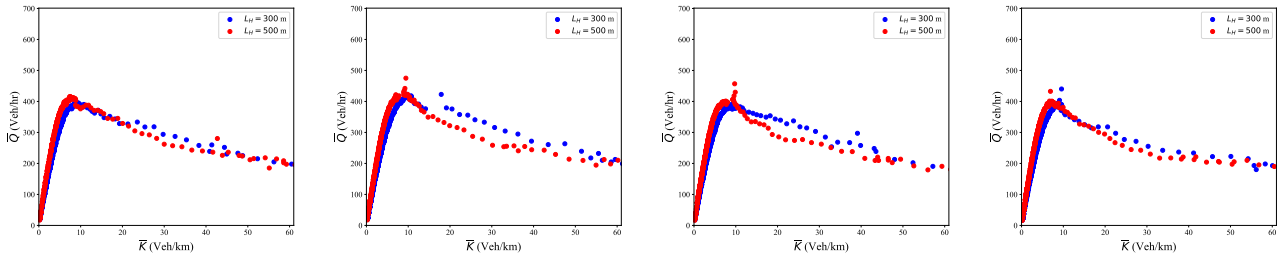

(a) $DBL = 1$ **(b)** $DBL = 2$ **(c)** $DBL = 3$ **(d)** $DBL = 5$

Figure 5: *MFD of links where both lanes are available for cars. Network parameters:* $n = 11$.

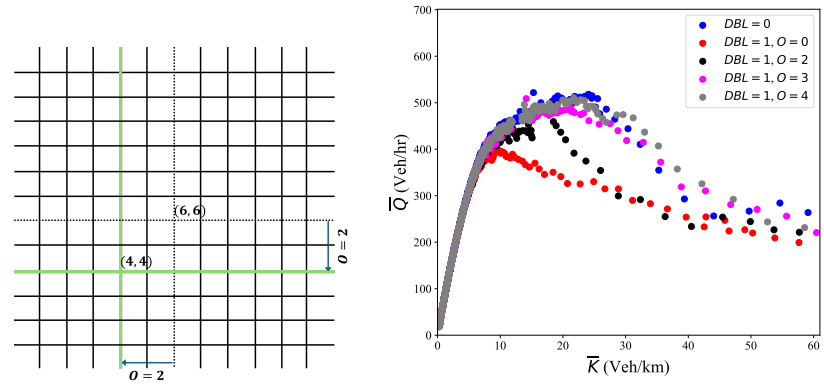

(a) *Example of non-uniform DBL placement* **(b)** *MFD*

Figure 6: *Effect of DBL offset on the MFD of the network available for cars. Network parameters:* $n = 11$, $L = 300$ m. *The variable O in legend represents the offset value.*

4 Conclusion

This study evaluates the impact of network configurations on the MFDs of bi-modal urban square grid networks, with a particular focus on intersections, block lengths, and the number and placement of DBLs. Through simulations in SUMO, we demonstrate that spatial heterogeneity introduced by DBLs significantly affects network performance. Links with DBLs restrict space for car traffic, altering the MFD shape and limiting the effectiveness of traditional spatially aggregated metrics, such as intersection density, in capturing the resulting variations in network capacity and critical density.

These findings emphasize the importance of developing spatially aware topology quantification metrics to account for the influence of multimodal interactions on MFDs. Such metrics can facilitate the development of better MFD prediction tools for multimodal transportation networks. Future research should extend these analyses to more complex and irregular network topologies and investigate additional multimodal factors, such as mixed-traffic conditions and dynamic traffic control strategies.

References

Ambühl, L. and Menendez, M. (2016). Data fusion algorithm for macroscopic fundamental diagram estimation. *Transportation Research Part C: Emerging Technologies*, 71:184–197.

Buisson, C. and Ladier, C. (2009). Exploring the Impact of Homogeneity of Traffic Measurements on the Existence of Macroscopic Fundamental Diagrams. *Transportation Research Record*, 2124(1):127–136.

Geroliminis, N. (2015). Cruising-for-parking in congested cities with an MFD representation. *Economics of Transportation*, 4(3):156–165.

Geroliminis, N. and Daganzo, C. F. (2008). Existence of urban-scale macroscopic fundamental diagrams: Some experimental findings. *Transportation Research Part B: Methodological*, 42(9):759–770.

Gu, Z., Safarighouzhdi, F., Saberi, M., and Rashidi, T. H. (2021). A macro-micro approach to modeling parking. *Transportation Research Part B: Methodological*, 147:220–244.

Gupta, N., Patil, G. R., and Vu, H. L. (2023). Simple abstract models to study stability of urban networks with decentralized signal control. *Transportation Research Part B: Methodological*, 172(June 2023):93–116.

Gupta, N., Patil, G. R., and Vu, H. L. (2024). Efficacy of decentralized traffic signal controllers on stabilizing heterogeneous urban grid network. *Communications in Transportation Research*, 4:100137.

Haddad, J., Ramezani, M., and Geroliminis, N. (2013). Cooperative traffic control of a mixed network with two urban regions and a freeway. *Transportation Research Part B: Methodological*, 54:17–36.

Johari, M., Keyvan-Ekbatani, M., Leclercq, L., Ngoduy, D., and Mahmassani, H. S. (2021). Macroscopic network-level traffic models: Bridging fifty years of development toward the next era. *Transportation Research Part C: Emerging Technologies*, 131:103334.

Keyvan-Ekbatani, M., Papageorgiou, M., and Papamichail, I. (2013). Urban congestion gating control based on reduced operational network fundamental diagrams. *Transportation Research Part C: Emerging Technologies*, 33:74–87.

Knoop, V. L., de Jong, D., and Hoogendoom, S. P. (2014). Influence of Road Layout on Network Fundamental Diagram. *Transportation Research Record*, 2421(1):22–30. MFD_NetworkStructure_Knoop2014.

Knoop, V. L., Hoogendoorn, S. P., and Van Lint, J. W. C. (2012). Routing Strategies Based on Macroscopic Fundamental Diagram. *Transportation Research Record*, 2315(1):1–10.

Leclercq, L., Chiabaut, N., and Trinquier, B. (2014). Macroscopic Fundamental Diagrams: A cross-comparison of estimation methods. *Transportation Research Part B: Methodological*, 62:1–12.

Li, Y., Mohajerpoor, R., and Ramezani, M. (2021). Perimeter control with real-time location-varying cordon. *Transportation Research Part B: Methodological*, 150:101–120.

Loder, A., Ambühl, L., Menendez, M., and Axhausen, K. W. (2019). Understanding traffic capacity of urban networks. *Scientific Reports*, 9(1):16283.

Lu, W., Liu, J., Mao, J., Hu, G., Gao, C., and Liu, L. (2020). Macroscopic Fundamental Diagram Approach to Evaluating the Performance of Regional Traffic Controls. *Transportation Research Record*, 2674(7):420–430.

Mühlich, N., Gayah, V. V., and Menendez, M. (2015). Use of Microsimulation for Examination of Macroscopic Fundamental Diagram Hysteresis Patterns for Hierarchical Urban Street Networks. *Transportation Research Record*, 2491(1):117–126.

Ortigosa, J., Menendez, M., and Tapia, H. (2015). Study on the number and location of measurement points for an MFD perimeter control scheme: a case study of Zurich. *EURO Journal on Transportation and Logistics*, 3(3):245–266.

Simoni, M. D., Pel, A. J., Waraich, R. A., and Hoogendoorn, S. P. (2015). Marginal cost congestion pricing based on the network fundamental diagram. *Transportation Research Part C: Emerging Technologies*, 56:221–238.

Taillanter, E., Schadschneider, A., and Barthelemy, M. (2024). Structure of road networks and the shape of the macroscopic fundamental diagram. *Physical Review E*, 109(1):014314.

Xu, G. and Gayah, V. V. (2023). Non-unimodal and non-concave relationships in the network Macroscopic Fundamental Diagram caused by hierarchical streets. *Transportation Research Part B: Methodological*, 173:203–227.

Yildirimoglu, M. and Geroliminis, N. (2014). Approximating dynamic equilibrium conditions with macroscopic fundamental diagrams. *Transportation Research Part B: Methodological*, 70:186–200.

Zhang, L., Garoni, T. M., and de Gier, J. (2013). A comparative study of Macroscopic Fundamental Diagrams of arterial road networks governed by adaptive traffic signal systems. *Transportation Research Part B: Methodological*, 49:1–23.

Zhang, L., Yuan, Z., Yang, L., and Liu, Z. (2020). Recent developments in traffic flow modelling using macroscopic fundamental diagram. *Transport Reviews*, 40(6):689–710.

Zhang, Z., Parr, S. A., Jiang, H., and Wolshon, B. (2015). Optimization model for regional evacuation transportation system using macroscopic productivity function. *Transportation Research Part B: Methodological*, 81:616–630.

Zheng, N., Waraich, R., Axhausen, K., and Geroliminis, N. (2012). A Dynamic Cordon Pricing Scheme combining a Macroscopic and an Agent-based traffic Models. *Transportation Research Part A: Policy and Practice*, 46(8):1291–1303.